

Attachment 2

OCAN080201

Use of Metamic® In Fuel Pool Applications



Holtec Center, 555 Lincoln Drive West, Marlton, NJ 08053

Telephone (856) 797-0900

Fax (856) 797-0909

USE OF METAMIC[®] IN FUEL POOL APPLICATIONS

Holtec Report No.: HI-2022871

Holtec Project No.: GENERIC

Report Category: A

Report Class: Safety Related

NON-PROPRIETARY VERSION

COMPANY PRIVATE

This document is proprietary and property of Holtec International. It is to be used only in connection with the performance of work by Holtec International or its designated client and subcontractors. Reproduction, publication and representation, in whole or in part, for any purposes by any other party is expressly forbidden.

Summary of Revision

Revision 0: Original Issue

Revision 1: Editorial changes per verbal discussions with the client. All changes are indicated by revision bars in the report. No conclusions were changed.

CONTENTS, HOLTEC INTERNATIONAL REPORT HI-2022871

1.0	INTRODUCTION AND SUMMARY	1
2.0	THE MANUFACTURE OF METAMIC®	4
2.1	PROCESS DESCRIPTION	
2.2	IMPORTANT PROCESS VARIABLES AND THEIR CONTROL	
3.0	METAMIC® COMPOSITION AND PHYSICAL PROPERTIES	5
3.1	COMPOSITION	5
3.2	PHYSICAL PROPERTIES AND TESTING	6
3.2.1	SHORT-TERM ELEVATED TEMPERATURE TESTING	6
3.2.2	LONG-TERM ELEVATED TEMPERATURE TESTING	7
3.2.3	RESULTS OF EARLIER TESTING	9
4.0	CORROSION TESTING OF METAMIC®	11
4.1	COUPON DESCRIPTIONS AND PURPOSES	12
4.2	TEST RESULTS	13
4.3	TEST CONCLUSIONS	15
5.0	RESISTANCE OF METAMIC® TO RADIATION DAMAGE	16
6.0	ADDITIONAL METAMIC® PROPERTIES DATA	19
7.0	COMPARISON: METAMIC® AND BORAL®	21
8.0	CONCLUSIONS	23
9.0	REFERENCES	24

APPENDIX A	TECHNICAL ASSESSMENT OF THE B ₄ C DISTRIBUTION IN METAMIC®	
------------	---	--

1.0 INTRODUCTION AND SUMMARY

The purpose of this topical report is to demonstrate that Metamic[®] is a desirable material for use as a neutron absorber in reactor fuel pool applications. The report will show that the properties of Metamic ensure it will perform reliably in fuel pools containing either deionized water (for boiling water reactors – BWRs) or in fuel pools containing borated water (for pressurized water reactors – PWRs).

Metamic is a fully-dense, discontinuously-reinforced, metal matrix composite material. It consists of a high-purity Type 6061 aluminum (Al 6061) alloy matrix reinforced with Type 1 ASTM C-750 isotopically-graded boron carbide (B_4C). This composite material, produced by Metamic LLC in Lakeland, Florida, may be extruded into a variety of product forms ranging from sheets and plates to angles, channels, round tubes, square tubes, and other cross-sections.

A natural application for Metamic in plate form is its use in high density fuel storage racks. In this application, the Metamic plates, or sheets, are placed between the cells of the storage racks and function as efficient thermal neutron absorbers. To ensure its satisfactory performance in the environments that exist in spent fuel pools, Metamic has been subjected to many tests that mimic the conditions to which the material will be exposed in actual service. The research and development (R&D) programs on Metamic, carried out by Metamic LLC, Northeast Technology Corporation (NETCO), and Holtec International (Holtec), show the material to be a stable, corrosion-resistant, cost-effective neutron absorber whose performance in fuel storage pools will be superior to that of materials currently employed. This report presents data on the composition, manufacture, physical properties, corrosion resistance, radiation resistance, and neutron-absorption characteristics of Metamic. In addition, the important characteristics of Metamic and Boral[®] are compared.

The development and testing of Metamic began as an in-house project at the Reynolds Metals Company and continued at California Consolidated Technology, Inc. (CCT).¹ In addition, the Electric Power Research Institute (EPRI) has been involved in the evaluation of the material.² The continuing testing efforts are under the cognizance of the manufacturer (Metamic LLC) and the design and construction organization (Holtec) that is specifying the material as the neutron poison in nuclear fuel racks.

The testing to which Metamic has been subjected includes the following:

- Short term (48 hour) elevated temperature (900°F) testing;
- long term elevated temperature (750°F) testing for times in excess of one year;
- accelerated corrosion testing (195°F) for times in excess of one year;
- accelerated radiation testing at exposures up to 1.5×10^{11} rads gamma;
- mechanical properties testing at temperatures up to 900°F; and
- neutron transmission testing of coupons before and after corrosion testing.

In tests that involved immersion of Metamic in water, parallel investigations were carried out in deionized water and in borated water. In addition to the Metamic properties determined by the testing listed above, the distribution of B_4C -- a characteristic as important in an absorber material as corrosion resistance is -- has been technically evaluated, as reported in Appendix A.

Metamic can be supplied in either mill-finish or anodized form, so mill-finish Metamic and anodized Metamic were included in the test programs, as was mill-finish 6061 aluminum alloy without B_4C . Since Metamic also can be produced in different compositions -- that is, with different loadings of B_4C -- samples containing different percentages of B_4C were evaluated in the tests. Past programs principally included samples with 15 wt.% B_4C and samples with 31 wt.% B_4C , while tests currently planned include samples with 40 wt.% B_4C .

The accelerated corrosion testing of Metamic was carried out in two media: deionized water to simulate BWR pool conditions, and deionized water containing 2500 ppm boron as boric acid to simulate PWR pool conditions. Mill finish and anodized coupons containing 15 wt.% and 31 wt.% B_4C were placed in each simulated pool environment. The tests showed the deionized water was a harsher environment for Metamic than was the borated water.

Neutron transmission tests were carried out on archive coupons and on coupon samples before those samples were placed in 1) 200°F deionized water and 2) 200°F deionized water containing 2500 ppm boron as boric acid. Intermediate transmission tests have been completed on the archive coupons and the coupons that had been exposed to the 200°F water environments. The tests show uniformity of absorption across the samples, as well as consistency in absorption between the archive coupons and the coupons exposed to the pool environments. The test

coupons have been returned to the water environments for additional exposure, after which they will be subjected to additional neutron transmission tests.

Testing has proved Metamic to be an excellent, desirable material for use as the neutron absorber in high-density fuel storage applications. When impurities deposited during the fabrication process have been cleaned from its surfaces – either by glass-beading of mill-finish material or by the cleaning that precedes anodizing -- Metamic is highly resistant to corrosion when exposed to the environments present in fuel storage pools. It is not subject to deformation or deterioration under environments far more hostile than those in fuel storage pools, and it remains an extremely consistent and effective neutron absorber.

The following sections of this report describe:

- the process and quality control employed in the manufacture of Metamic;
- the composition and properties of Metamic;
- the results of corrosion tests to which Metamic has been subjected;
- Metamic's resistance to radiation damage;
- additional mechanical properties data for Metamic;
- the qualities of Metamic vs. those of Boral; and
- the performance of Metamic in fuel pools.

In addition, the appendix to the report presents a technical assessment of the distribution of B_4C particles in Metamic. The appendix was extracted from information presented in Ref. 1. |

2.0 THE MANUFACTURE OF METAMIC[®]

The information on the manufacturing process of METAMIC is proprietary to Metamic LLC. Due to the mutual proprietary information withholding agreement between Metamic Inc. and Holtec International, this section is not presented in this version of the report.

3.0 METAMIC® COMPOSITION AND PROPERTIES

3.1 COMPOSITION

A Reynolds Metal Company data sheet⁵ shows the relationships between the 6061 aluminum matrix and the B₄C “reinforcement” in Metamic for different B₄C contents, as well as the resulting densities of the composite material, as follows.

<u>Wt. % B₄C</u>	<u>Wt. % Al6061</u>	<u>Vol. % B₄C</u>	<u>Composite Density, gm/cm³</u>
4.68	95.32	5	2.691
9.40	90.60	10	2.682
14.14	85.86	15	2.673
18.92	81.08	20	2.664
23.73	76.27	25	2.655
28.57	71.43	30	2.646
33.45	66.55	35	2.637
38.36	61.64	40	2.628
43.30	56.70	45	2.619

A California Consolidated Technology specification for 40 wt.% Metamic called for high-purity aluminum powder and ASTM C 750 / Type 1 B₄C powder with the following compositions.

6061 Aluminum Powder (high purity)

<u>Element</u>	<u>Spec. Range</u>
Mg	0.080-1.20
Si	0.40-0.80
Cu	0.15-0.40
Fe	0.15 max.
Zn	0.25 max.
Ti	0.15 max.
Ni	50 ppm max.
Co	10 ppm max.
Mn	10 ppm max.
Cr	10 ppm max.
Other/each	0.05 max.
Others/total	0.15 max.

ASTM C 750 / Type 1 B₄C Powder

<u>Element</u>	<u>Spec. Range</u>
Total B	76.50 % min.
Total B+C	98.0% min.
B10	19.90±0.3a/o
HNO ₃ sol.B	0.59% max.
H ₂ O sol.B	0.29% max.
Si	0.50% max.
Fe	0.50% max.
Calcium	0.30% max.
Fluoride	25 ppm max.
Chloride	57 ppm max.

3.2 PHYSICAL PROPERTIES AND TESTING

The properties and behavior of Metamic have been established by a program in which many samples were subjected to elevated temperature testing. As reported in Refs. 1 and 2, there have been two elevated-temperature testing regimes, one short-term and the other long-term. In each regime, mill-finish and anodized rectangular coupons and mill-finish and anodized tensile coupons were tested, with each surface finish represented by 15 wt.% and 31 wt.% B₄C samples. Other tests, discussed separately in Section 6.0 of this report, were directed toward determining the mechanical properties of Metamic containing 40 wt.% B₄C.

3.2.1 SHORT-TERM ELEVATED TEMPERATURE TESTING

Metamic samples were exposed to a temperature of 900°F in an inert atmosphere for 48 hours. The samples consisted of rectangular coupons 2"x 4"x 0.075" and reduced-section tensile specimens. The samples were characterized before and after exposure to the elevated temperature. Test results are outlined in the following paragraphs.

Physical Appearance

The exposure caused some darkening of the surfaces of the 15 w/o mill-finish coupons, while the 31 w/o mill-finish coupons were only slightly darker after exposure than before. The appearance of the 15 w/o anodized coupons underwent only a possible slight darkening, and the 31 w/o anodized coupons looked about the same before and after testing.

Dimensions

The 31 w/o coupons show an extremely small (<0.05%) maximum change in length, only slightly more than the individual measurement uncertainty. The average thickness change for all 60 coupons was approximately 0.5%.

Density

There was no change in coupon density after 48 hours at 900°F.

Boron-10 Areal Density

Within the precision of the measurement, there was no change in Boron-10 areal density after 48 hours at 900°F.

Mechanical Properties

The pre-test and post-test mechanical properties are listed in the following table, with values taken directly from Refs. 1 and 2. Coupons not subjected to elevated temperatures were used for the pre-test data: results from these coupons establish baseline information for Metamic in the as-fabricated condition.

	<u>15 w/o B₄C</u>	<u>31 w/o B₄C</u>
<u>Pre-Test</u>		
Yield Strength, psi	21797 ± 2179	32937 ± 3132
Ultimate Strength, psi	33379 ± 1723	40141 ± 1860
Elongation, %	10.2 ± 1.1	1.8 ± 0.8
<u>Post-Test</u>		
Yield Strength, psi	21216 ± 1820	28744 ± 3246
Ultimate Strength, psi	34152 ± 1914	34608 ± 1513
Elongation, %	12.1 ± 1.2	5.7 ± 3.1

The results show yield strength and ultimate strength increase with increasing B₄C content, while the elongation decreases. These changes are consistent with the increase in the content of the harder material, and the trend continues as B₄C content is increased to 40%, as seen in Section 6.0 of this report.

Rockwell Hardness

Comparison of pre-test and post-test values showed that, within one standard deviation of the measured values, there was no change in Rockwell hardness of the 15 w/o or 31 w/o coupons (Rockwell E and Rockwell B, respectively).

3.2.2 LONG-TERM ELEVATED TEMPERATURE TESTING

Metamic samples were exposed to a temperature of 750°F in an air atmosphere. After 2133 hours, 4124 hours, and 6139 hours, the coupons were cooled to room temperature and subjected to non-destructive testing, then reinserted in the test environment. When the total test time had reached 8523 hours, the test coupons were subjected to non-destructive testing as well as destructive mechanical testing. Some coupons underwent neutron attenuation testing and density measurements. The samples were characterized before and after exposure to the elevated temperature. Test results are outlined in the following paragraphs.

Physical Appearance

All mill-finish coupons turned a darker color. The longer the coupons were at temperature, the darker and more uniform the color became. The color of the anodized coupons after exposure was similar to their color before exposure.

Dimensions

Within the precision of the measurements, there was no change in coupon length and width after 8523 hours at 750°F. On average, the coupons appeared to have increased very slightly in thickness – about 0.00015 inches.

Dry Weight

There was no significant change in coupon weight.

Boron-10 Areal Density

As determined by neutron attenuation testing, there was no change in the B-10 areal density after 8523 hours at 750°F.

Density

Within the precision of the measurements, there was no change in density after 8523 hours at 750°F.

Mechanical Properties

The pre-test and post-test mechanical properties are listed in the following table, data for which were taken directly from Refs. 1 and 2. The pre-test data resulted from tests on coupons not subjected to elevated temperatures, as was the case with the short-term coupons. Results from tests of these coupons establish baseline information for Metamic in the as-fabricated condition.

	<u>15 w/o B₄C</u>	<u>31 w/o B₄C</u>
<u>Pre-Test</u>		
Yield Strength, psi	22230 ± 2179	32937 ± 3132
Ultimate Strength, psi	33379 ± 1723	40141 ± 1860
Elongation, %	9.9 ± 1.1	1.8 ± 0.8
<u>Post-Test</u>		
Yield Strength, psi	20991 ± 3095	28995 ± 1689
Ultimate Strength, psi	34387 ± 1080	36952 ± 1204
Elongation, %	11.1 ± 0.5	2.8 ± 1.8

(Note the value of the pre-test yield strength for the 15 w/o B₄C seems inconsistent with the value given for the short-term pre-test: the values shown here are those that appear in Refs. 1 and 2.) As was the case in the short-term tests, the results show yield strength and ultimate strength increase with increasing B₄C content, while the elongation decreases. These changes are consistent with the increase in the content of the harder material and, as was the case with the short-term tests, the trend continues as B₄C content is increased to 40% (see Section 6.0).

Comparison of the pre-test and post-test values shows that, within one standard deviation, there is no change in any of the mechanical properties of the 15 w/o B₄C Metamic. This was verified by applying a t-test to the mean of the data and an f-test to the variance (the square of the standard deviation). This showed there was no statistically significant change in the yield or ultimate strength, and that there is a small but statistically significant increase in elongation.

The 31 w/o coupons showed a very small, but detectable, decrease in the yield and ultimate strength and an increase in elongation. A decrease in strength and an increase in elongation are consistent with annealing. Application of t-tests to the means of the measured values, and f-tests to the variances, support a conclusion that the higher-loaded coupons underwent some annealing of residual cold work. (In non-technical terms, the residual cold work results from the processes the material is subjected to during the fabrication of the coupons, and it has the effect of “tightening” the structure of the material. The annealing releases the energy associated with the cold work and “relaxes” the coupon material. The relaxed material has less strength, and it “stretches” better.)

Rockwell Hardness

There was some variability in the post-test data. However, comparison of the pre-test and post-test values showed that, within one standard deviation of the measured values, there was no change in Rockwell hardness of the 15 w/o or 31 w/o coupons (Rockwell E and Rockwell B, respectively).

3.2.3 RESULTS OF EARLIER TESTING

Prior to the programs described above, the coefficient of thermal expansion had been determined⁶ for several Metamic B₄C loadings, giving the values that follow. Note the values of the coefficient are given as functions of the *volume* loading of B₄C.

<u>B₄C Volume, %</u>	<u>Expansion Coefficient/°F x 10⁶</u>
0	13
12	11
26	8.5
40	6.5

The coefficient of thermal expansion is one of the mechanical properties of interest for all solid materials. It is used when determining ultimate sizes of fabricated forms and when evaluating differential thermal expansion between two or more solids of different compositions.

4.0 CORROSION TESTING OF METAMIC®

An accelerated test program was undertaken^{1,2} to assess the corrosion performance of Metamic in fuel storage pools. Mill-finish and anodized Metamic coupons were tested in 1) deionized water, to simulate BWR pool conditions, and 2) deionized water containing 2500 ppm boron as boric acid, to simulate PWR pool conditions. Both tests were conducted with the water temperature controlled at 195°F, and the duration of testing was 9020 hours (greater than one year). In addition to Metamic coupons containing 15 w/o and 31 w/o B₄C, mill-finish 6061 Al coupons were included in the tests.

The elevated temperature of the tests, substantially higher than the temperatures reached by fuel pool water, was selected to accelerate any corrosion that might occur at the lower temperatures in which Metamic would see service.

Several types of potential corrosion were evaluated in each water environment, and the coupons were pulled and examined at three interim times during the testing -- 2133, 4124, and 6140 hours -- as well at the completion of the tests (9020 hours).

The total number of coupons tested was 320, and their distribution among the various kinds of testing was as shown in the following table.

<u>Sample Type</u>	<u>Deionized Water</u>		<u>Boric Acid</u>	
	<u>15 w/o B₄C</u>	<u>31 w/o B₄C</u>	<u>15 w/o B₄C</u>	<u>31 w/o B₄C</u>
Mill-Finish Metamic				
General	10	10	10	10
Crevice	10		10	
Galvanic	10		10	
Weld	10		10	
Encapsulated	10	10	10	10
Anodized Metamic				
General	10	10	10	10
General w/scratches	10		10	
Crevice	10		10	
Galvanic	10		10	
Weld	10		10	
Encapsulated	10	10	10	10
Mill-Finish 6061		10		10

4.1 COUPON DESCRIPTIONS AND PURPOSES

The mill-finish Metamic coupons, the anodized Metamic coupons, and the 6061 aluminum coupons were rectangles measuring 2 in. x 4 in. x 0.075 in. thick (nominal).

General Coupons

The purpose of these coupons was to determine the rate at which a uniform oxide film formed. The coupons were precision weighed prior to testing, and when testing had been completed, they were subjected to a nitric acid wash, were dried, and were precision weighed again.

General Coupons with Scratches

Scratches were applied to the anodized coupons to simulate handling scratches that would be incurred during assembly/fabrication of fuel racks. The corrosion performance of these scratched coupons was assessed by optical microscopy.

Crevice Coupons

Each of these coupons had two 0.250-in. holes; the holes were used to attach two crevice-forming Teflon washers by 6061 aluminum machine screws and an insulating Teflon shoulder washer. The Teflon washers were used for the test configuration only; neither they, nor any other Teflon, will be used in fuel pool applications.

Galvanic Coupons

Because of its good mechanical properties, Metamic may find fuel pool applications in which it is not sheathed. In this case, LWR fuel assemblies may contact the Metamic. Consequently, bi-metallic coupons were prepared with Metamic and the following metals:

- 304-L stainless steel;
- Inconel 718; and
- Zircaloy 2.

The two metals comprising each couple were fastened to each other mechanically. Inspection of the galvanic coupons was by optical microscopy thickness and dry weight measurements.

Weld Coupons

These coupons contained a transverse butt weld made with a series 4000 alloy. The weld coupons were inspected by optical microscopy, with acid cleaning employed as needed.

Encapsulated Coupons

Each of these coupons was enclosed in a volume created by stainless steel plates on each side of a peripheral, "picture frame" plate. Limited flow was permitted through the coupon-containing central void to simulate the semi-stagnant condition encountered by the neutron absorber in some racks.

Aluminum 6061 Alloy Coupons

The material specification for these coupons was identical to that of the 6061 matrix of the Metamic coupons. The 6061 coupons, which were not anodized, were included to serve as a baseline for comparison if the Metamic coupons performed unexpectedly.

4.2 TEST RESULTS

The following paragraphs summarize results of the tests for each coupon type. Although intermediate results were obtained, the following summaries pertain to the final, 9020-hour-exposure results.

General Coupons

In both the BWR and the PWR tests, the mill-finish coupons suffered localized pitting corrosion, while most of the anodized coupons did not. The results of the general corrosion testing can be summarized as follows.

- The 15 w/o mill-finish coupons in the simulated BWR conditions showed the greatest pitting. Backscatter scanning electron microscopy showed impurities on the coupon surfaces, and these impurities were determined to have been deposited during manufacture of the coupon material.
- The 31 w/o mill-finish coupons were cleaned by glass beading after manufacture (the technique was not available when the material for the 15 w/o coupons was made); these coupons underwent essentially no weight change and showed very limited pitting compared to the 15 w/o coupons.
- The anodized coupons had been chemically cleaned to remove impurities prior to anodizing, and most of these coupons showed no pitting corrosion. Three of the anodized coupons showed limited local corrosion pits. All anodized coupons underwent essentially no weight change.

The experience with the general coupons emphasizes the need to clean the surfaces of the Metamic thoroughly to remove any contaminants.

General Coupons with Scratches

Qualitative optical microscopy on the scratched anodized coupons showed the scratched regions appeared to be developing a uniform oxide film where the anodic layer was initially missing. No accelerated corrosion effects were noted on the scratch areas or on other areas of the coupons.

Crevice Coupons

Thickness measurements gave indications the 15 w/o mill-finish coupons tended to develop a thicker oxide film under the crevice-forming washers than did the 15 w/o anodized coupons. Data for the 31 w/o coupons of each type are not available, but it is thought there would be no difference in performance of the two, inasmuch as both types had been well-cleaned before exposure.

Galvanic Coupons

The mill-finish coupons exhibited various degrees of localized pitting characteristic of crevice and galvanic-assisted corrosion. The anodized coupons showed no weight change, and metallographic examination did not reveal local pitting except for that on one 304-Metamic couple. It is speculated the pitting was caused by surface contamination. Again, surface cleaning appears to be the controlling factor.

Weld Coupons

The 15 w/o mill-finish weld coupons experienced substantial corrosion in the weld areas. It is speculated the heavy pitting corrosion in the weld metal could have been caused by impurities in the 4000 series alloy used for TIG welding. The 15 w/o anodized weld coupons did not show any corrosion on either the base metal or weld.

Encapsulated Coupons

Neither the mill-finish nor the anodized coupons, each with 15 w/o and 31 w/o samples, showed a weight change. Metallographic examination of the coupons showed limited, localized pitting corrosion of the mill-finish coupons, but none on the anodized coupons.

Aluminum 6061 Alloy Coupons

All 6061 coupons were mill finish, and the corrosion characteristics of these coupons differed somewhat from that of the Metamic coupons. Generally, the 6061 coupons in both the BWR and

PWR tests were covered by a light, uniform oxide. In the PWR tests only, each of the mill finish Al 6061 coupons had one or two very large pits on each side.

4.3 TEST CONCLUSIONS

The results obtained by broad-scope, accelerated, corrosion testing of Metamic for a period greater than one year demonstrate the excellent corrosion resistance of properly-prepared Metamic in environments that are significantly more hostile than those encountered in fuel storage pools.

The Metamic samples that underwent surface cleaning (glass-beading or anodizing) prior to corrosion testing performed much better than the mill-finish specimens, as evidenced by the absence of pits in the cleaned material. This can be explained by examining how Metamic sheets are produced. In the extrusion process that precedes hot rolling, the extremely-hard B_4C particles in the Metamic cause some erosion of the extrusion die. The eroded bits from the die are deposited on the surfaces of the extruded billet and remain on the surfaces of the final, hot-rolled product. Either glass-beading or the chemical cleaning associated with anodizing removes the impurities and greatly improves the performance of the Metamic in terms of pit formation. In practice, when placed in the aqueous environment of the fuel pool, properly-cleaned, mill-finish Metamic will develop the surface layer of hydrated aluminum oxide comparable to, and providing the same protection as, the surface of anodized material.

The presence of B_4C , an extremely hard, chemically-inert material, affects the physical properties of Metamic but does not affect the chemical properties. Thus, the corrosion of Metamic follows that of the 6061 aluminum and is independent of the B_4C content.

Metamic specified as the neutron-poison material in fuel storage racks should have either a glass-beaded or a chemically-cleaned surface finish.

5.0 RESISTANCE OF METAMIC[®] TO RADIATION DAMAGE

Metamic has been subjected to intensive levels of gamma radiation and to lesser levels of fast neutron radiation.^{1,2} A number of Metamic packets were placed in a specially designed and custom fabricated Metamic canister at the Ford Nuclear Reactor (FNR) at the University of Michigan. The canister serves as a thermal neutron shield to minimize the amount of thermal neutron energy deposited in the coupons. The canister has inlet and outlet cooling ports, designed with baffles, to preclude neutron streaming.

The Metamic radiation canister is being irradiated at the core face centerline, where it accumulates gamma energy deposition at the rate of 4.5×10^9 rads per ten-day operating cycle of the FNR. Every 2.5 days of the operating cycle, the canister is rotated one-quarter turn so all the coupons contained within receive approximately the same exposure.

The canister contains rectangular coupons and tensile coupons (reduced section). The total number of coupons being tested is 144, including 12 coupons of aluminum 6061. The coupons are arranged in 12 packets of 12 each; six of the packets have been removed from the canister. The remaining packets continue to be irradiated.

The coupons that have been removed received gamma doses ranging from 4.5×10^9 rads (for the first packet removed) to 1.5×10^{11} rads (for the sixth packet removed). The dose to the sixth packet is roughly equivalent to the exposure Metamic would receive in 40 years of actual fuel rack service, and is far below the exposures that cause radiation damage in metals. The fast neutron exposures to the Metamic in the six packets were in the range 1.7×10^{18} nvt to 5.8×10^{19} nvt.

Mechanical properties were determined for the coupons in the fifth packet removed, with the following results, which are taken from Refs. 1 and 2. The gamma radiation dose for the coupons in the fifth packet, whose mechanical properties are given in the following table, is stated^{1,2} to have been 7.5×10^{10} rads. (Note that there appears to be an inconsistency in the value given for the ultimate strength of the pre-test, 15 w/o B₄C Metamic when compared to the value given earlier for the long-term temperature test. Regardless of this, the conclusions based on the test results remain valid.)

	<u>15 w/o B₄C</u>	<u>31 w/o B₄C</u>
<u>Pre-Test</u>		
Yield Strength, psi	22230 ± 2179	32937 ± 3132
Ultimate Strength, psi	33889 ± 1723	40141 ± 1860
Elongation, %	9.9 ± 1.1	1.8 ± 0.8
<u>Post-Test (7.5x10¹⁰ rads)</u>		
Yield Strength, psi	21115 ± 158	28146 ± 1463
Ultimate Strength, psi	31954 ± 217	28872 ± 411
Elongation, %	9.3 ± 0.5	3.3 ± 2.0

Examination of the coupons that have been tested to these radiation levels leads to the following observations.

- Metamic exhibits excellent dimensional stability after irradiation.
- There was no change in Boron-10 areal density.
- Within the accuracy of the measurements, the mechanical properties of the 15 w/o B₄C coupons did not change.
- The 31 w/o coupons experienced an apparent decrease in ultimate strength and an increase in elongation. The changes may be due to temperature effects rather than radiation effects: during irradiation, energy deposition in the coupons may cause them to experience a significant rise in temperature. In any case, the use of Metamic in wet storage applications does not require the material to possess high strengths.
- There was no change in Rockwell hardness.

Embrittlement of Metamic in wet storage applications is not a concern. Metallic materials, such as Metamic, typically require much higher radiation doses than the levels that will be experienced in fuel pools and exposure durations significantly greater than the lifetimes of fuel storage racks for embrittlement.

Radiation and an aqueous environment do not couple to produce a synergistic effect on the corrosion of metals. The use of aluminum and other metals in wet, high-radiation environments for many years (in reactors, fuel storage facilities, test cells, etc.) has shown the corrosion behaviors of the metals are not affected by radiation. Consequently, no corrosion tests were performed on the Metamic samples following their irradiation, and no tests are planned. Radiation has no effect on the corrosion rate of Metamic.

Free radicals created by high gamma radiation fields will have no effect on the surfaces of Metamic. The performance of Boral in high-gamma fields has shown that free radicals, if present, have no effect on the surface of aluminum.

6.0 ADDITIONAL METAMIC PROPERTIES DATA

California Consolidated Technology, Inc. had mechanical-properties tests performed on Metamic containing 40 w/o B₄C. The tests, performed in air, used Metamic from CCT manufacturing lot #108 and were carried out at room temperature, as well as at elevated temperatures. All testing was in accordance with the latest revisions of applicable ASTM International specifications. The results were as follows.

<u>Test Temperature, °F</u>	<u>Yield Strength, psi</u>	<u>Ultimate Strength, psi</u>	<u>Elongation, %</u>
Room Temperature	30,013	44,282	2.0
Room Temperature	28,600	35,800	2.0
Room Temperature	30,100	44,700	1.0
200	28,700	40,600	2.0
200	27,500	40,200	4.0
200	24,700	36,500	2.5
500	14,700	18,300	4.5
500	14,700	18,100	3.5
500	15,276	20,458	2.5
800	6,300	7,700	1.5
800	5,800	6,800	2.0
800	8,100	10,500	1.0
900	2,800	3,600	4.0
900	3,200	4,000	4.0
900	3,848	4,507	1.0

The room-temperature results shown above for the Metamic 40 w/o B₄C are comparable to the pre-test results given for Metamic 31 w/o B₄C in Section 3.0 of this report. This similarity in performance shows there will not be large changes in properties between the two Metamics containing the heavier loadings of B₄C (31 w/o and 40 w/o).

CCT also had coefficient of thermal expansion tests performed on the 40 w/o Metamic at elevated temperatures. There are no values directly comparable to the room-temperature coefficient given in Section 3.2.3 for 40 *volume*-percent Metamic, but the values given in the table on the following page are consistent.

Metamic B₄C Content

40 volume percent

40 weight percent

Expansion Coefficient/^oF x 10⁶

6.5 at room temperature

6.57 at 200 F.

7.0 COMPARISON: METAMIC® AND BORAL®

The properties and behavior of Metamic can be compared to those of Boral as a neutron poison in fuel storage pool environments. The following table provides information on each material.

	<u>METAMIC</u>	<u>BORAL</u>
Metal	Aluminum 6061	Aluminum 1100
Neutron Poison Material	Boron Carbide (B ₄ C)	Boron Carbide (B ₄ C)
Beginning Materials	Powders	Powders and Plate
Initial Shape/How Formed	Billet/Cold isostatic pressing	Ingot/Al box contains powder
B ₄ C Particle Size, microns	5 to 9	~ 40
B ₄ C Content, %	40 throughout	44 in matrix only
Uncertainty in B ₄ C Content, %	± 0.5	± 8.0
B ₄ C Distribution	Uniform throughout	Uniform in matrix
Treatment	Sintering and degassing	Heating
Forming into Plates	Extruding and hot rolling	Hot rolling
Surface Finishes	Mill, glass beaded, or anodized	Mill or anodized
Yield Strength, psi	21,000 – 33,000	9,000 – 12,000
Elongation, %	1.8 – 12.1	0.1 – 0.7
Weldability	Good with friction welding	Poor: heat-affected zone pits
Corrosion Resistance in Hot Water and Hot Borated Water	Very good	Very good
Resistance to Radiation Damage	Very good	Very good
Organic content,%	0	0

The blistering of Boral that has been seen to occur occasionally in fuel pool applications is caused by the generation of hydrogen gas within the central layer, or matrix, of the laminated material. The gas is generated by the reaction of the aluminum of the matrix with water that has entered the

porous matrix and then been sealed in place by oxidation of the escape paths from the laminate. The gas is unable to escape, and the local pressures it generates causes blisters to occur in the outer layers of pure aluminum. Metamic is not subject to blister formation, for it is a homogeneous material with no open porosity.

Despite the fact that the Type 1100 aluminum in Boral is not as corrosion-resistant as the marine-qualified Type 6061 aluminum of Metamic, Boral performed well for many years in university reactors. The following quotations from operators of university reactors make a very strong, indirect argument for the sustained satisfactory performance of Metamic, a relatively-new material whose suitability for use under heated water, in high radiation fields, exceeds that of Boral. The nominal operating temperatures for the university reactors named below range from 97F to 120F, temperatures similar to those that exist in fuel storage pools. The use of Boral in the cores of nuclear reactors exposes the material to radiation fields much stronger than those in fuel storage pools.

The Director of the Washington State University Reactor made the following statement regarding the Boral in his facility: "After 31 year's service, the original Boral safety rods are still performing well. They look fine."⁸

At the University of Wisconsin, the reactor continued to use its original Boral control blades 31 years later. The Boral blades "...are doing fine, with no indication of deterioration." The blades were subjected to detailed annual inspections, including micrometer determination of thicknesses. Boral was also used in beam-port shutters, thermal column liners, and a thermal column door. In some of these applications, the Boral could not be inspected, but continued "...to do the job."⁹

At the Rhode Island Nuclear Research Center reactor, the Boral in the one regulating rod and the four control blades – components that had been operating for 28 years in water at 120F – "...has performed well, with no evidence of swelling, cracking, or other degradation observed during brief annual inspections. The worth has not changed."¹⁰

Although Boral has been shown to perform adequately in numerous applications, the comparison given in the table on the preceding page shows clearly that Metamic is an even more desirable material. It is stronger than Boral, its B₄C particle size is much smaller than that of Boral, and the uncertainty in B₄C content is much less in the Metamic.

8.0 CONCLUSIONS

Extensive past testing, continuing test programs, and a comparison with Boral show clearly the superiority of Metamic as a neutron poison material in nuclear fuel wet-storage applications.

Based on an aluminum alloy (Type 6061) known for its strength and its corrosion resistance in marine applications, Metamic contains a uniform distribution of B_4C – B_4C with an extremely small particle size. Not only is the Metamic B_4C particle size less than 25% of the particle size of the B_4C in Boral, the content of B_4C in Metamic is known within ± 0.5 %; the content in Boral is known no better than ± 8.0 %.

Although the strength of the neutron poison material is not a primary consideration in current wet-storage rack design, the use of Type 6061 aluminum in the manufacture of Metamic insures it is a rugged metal. This is borne out by the excellent results from the numerous tests to which Metamic samples with B_4C contents up to 40% have been subjected. Furthermore, if future designs envision Metamic performing a structural function as well as its role as the neutron poison, friction welding of the Metamic may simplify the design and construction of the racks.

Corrosion tests on hundreds of Metamic samples for a period greater than one year and at a temperature far hotter than the temperatures Metamic will experience in wet storage applications show the material does not corrode or pit when its surfaces are properly cleaned. The surface of mill-finish Metamic requires glass-bead cleaning or the chemical cleaning typically used for the anodizing process. When cleaned by glass-beading and then placed in water, the Metamic surfaces develop an oxide surface layer that provides the same protection as an anodized finish.

The majority of tests have been performed on Metamic with B_4C contents of 15 w/o and 31 w/o. However, there have been sufficient tests on 40 w/o Metamic to confirm that the extrapolation of results from tests of material with lower B_4C contents is reasonable and consistent. Increasing the boron carbide content affects the mechanical properties, not the corrosion and pitting resistance, for the boron carbide is inert. The corrosion and pitting behavior remains the same as that of the base material, Type 6061 aluminum, and the behavior of that marine-qualified alloy is very good.

Metamic is well tested and highly desirable, and its use as the neutron poison in wet storage applications will result in performance superior to that of materials specified in the past.

9.0 REFERENCES

1. *METAMIC* Qualification Program For Nuclear Fuel Storage Applications, Final Test Results*, Draft Report NET 152-03, Prepared for California Consolidated Technology, Inc. by Northeast Technology Corporation (Undated confidential draft).
2. *Qualification of METAMIC* For Spent-Fuel Storage Applications*, Report 1003137, EPRI, Palo Alto, CA, October 2001.
3. Metamic LLC Quality Assurance Program, Rev. 0, April 1, 2002 (Proprietary).
4. Metamic LLC Quality Control Procedures (Route Cards), Various revisions, Various dates (Proprietary).
5. *Volume Loading vs. Weight Percent of Various Reinforcement Materials in AIMMC's*, Reynolds Metal Company Data Sheet, Undated.
6. *Expansion Coefficient As a Function of Boron Carbide Content for Aluminum Metal Matrix Composites*, Reynolds Metal Company Data Sheet, Undated.
7. Private communication, Tom Haynes, Metamic LLC, to Stanley E. Turner, Holtec International, June 2002.
8. Personal communication, Dr. Gerald Tripard, Director, Washington State University Reactor, to W. Mitchell, III, Holtec International, November, 1992.
9. Personal communication, R. J. Cashwell, Director, University of Wisconsin Nuclear Reactor, to W. Mitchell, III, Holtec International, November, 1992.
10. Personal communications, Wayne Simeneau, Assistant Director, Rhode Island Nuclear Science Center, to W. Mitchell, III, Holtec International, November 1992.

APPENDIX A TECHNICAL ASSESSMENT OF THE B₄C DISTRIBUTION IN METAMIC®

TECHNICAL ASSESSMENT OF THE B₄C DISTRIBUTION IN METAMIC®

1.0 Introduction

The neutron absorption properties of a sample of METAMIC® can be measured by its neutron *transmission ratio*, T . This is the ratio of the number of neutrons detected on the other side of the sample to the total number of neutrons incident upon the sample's face. The ¹⁰B in the B₄C constituent of METAMIC® is responsible for nearly all of the absorption, so the transmission is a measure of the amount of B₄C in the sample within the diameter of the neutron beam.

Measurements of the transmission ratio are expected to vary from measurement to measurement due to the Poisson statistics of the radiation detection process. Thus in measuring many different locations on a plate of METAMIC®, some amount of variance is expected. Because the Poisson variance can be computed analytically, this expected variance can be compared to the observed variance across the locations. If the observed variance substantially exceeds the expected variance, then there is evidence of either experimental error or variance in the B₄C loading of the METAMIC® sample. Careful experimentation and analysis can minimize the experimental error, so any significant excess variance is a good measure of non-uniformity of B₄C in METAMIC®. The distinction between global non-uniformity (e.g., from one side of the plate to the other, due to manufacturing processes) and local non-uniformity (e.g., non-uniform dispersion of the B₄C in the aluminum) can be made via multivariate regression analysis. Statistically significant trends would be indicative of global variation, while the absence of trends indicates local non-uniformity.

Not only should the variance be reasonably consistent with the Poisson statistical variance, but the location to location transmission ratios should be normally distributed and should not have any outliers. The Anderson-Darling and Cramér-von Mises statistical tests will be used to judge normality at an $\alpha=5\%$ level of significance. Plots will be used extensively to illustrate the results and note any outliers if they are observed.

Since sample thicknesses were also measured this data is presented as well. The thickness does not affect the uniformity of the B₄C loading, but it does impact the effectiveness of a METAMIC® sample at attenuating neutrons. This effectiveness can be quantified by the "areal density" of the sample - the mass of ¹⁰B per unit area of absorber. The areal density can be calculated by comparing the measured transmission ratio to a fit of areal density versus transmission ratio for standards of known areal density.

2.0 Experimental Method

The neutron transmission measurements were made in the Beam Hole Laboratory of the Breazeale Reactor Facility at the Pennsylvania State University. The Triga Reactor (with a rating of 1 MW_{th} (steady state)) is used as a source of neutrons. It is moved adjacent to a D₂O filled thermal column which, in turn, is adjacent to an air filled pipe running through the pool wall into the Beam Hole Laboratory. The pipe contains neutron collimators and baffles. The thermal column and collimators provide a mono-directional and nearly mono-energetic (thermal)

beam of neutrons in the Beam Hole Laboratory.

The neutron transmission ratio is determined by first measuring the neutron intensity with only a BF₃ detector in the beam. A specimen of METAMIC[®] is placed between the BF₃ detector and the beam to measure the intensity of thermal neutrons transmitted through the neutron absorber. A very thick neutron absorber is also placed between the detector and the beam to determine the "background" beam intensity. The background intensity is a measure of epi-thermal neutrons which pass through the absorber without being absorbed.

3.0 Analytical Development

With only a few exceptions, all detector counts were taken for 30 seconds. The exceptions were increased count times to provide enhanced accuracy with respect to the Poisson counting statistics very high B₄C loadings (leading to low count rates), as well as for the low count rate background counts. The background count rate was subtracted from every count rate.

The counts detected will vary as a function of the reactor power. Thus the counts from the power port are used to proportionately scale the count rate. Due to variations during manufacture the thicknesses of the samples are not uniform. Thus, for analyses of B₄C uniformity the thickness was also used to proportionately scale the count rate. While the thickness proportionality is not truly linear, the linear approximation is sufficient for the small deviations in thickness observed. The adjustments were applied as follows:

$$CR_{adj} = \left(CR \cdot \frac{P_{nominal}}{P} - CR_{background} \right) \cdot \frac{t}{t_{nominal}}$$

where CR is the count rate, P is the power port count, and t is the thickness. The thickness ratio term is only applied for analyses of B₄C uniformity. The transmission ratio is then computed as

$$T = \frac{CR_{adj}}{CR_{adj}^0}$$

where CR_{adj}^0 is the unattenuated count rate, adjusted as above. The uncertainty in the transmission ratio due to the Poisson statistics is computed by applying the propagation of error formula to the above equations.

The ¹⁰B areal density, Δ_A , of a sample is the mass of ¹⁰B per unit area of the sample available to attenuate the neutron beam. Given the B₄C loading and the thickness of a sample, its areal density can be calculated. According to the physics of neutron absorption, the ¹⁰B in a sample will exponentially attenuate a monoenergetic beam of neutrons across its thickness according to its areal density. Thus, for a theoretical monoenergetic beam, the areal density should be linearly related to the natural log of the transmission ratio. A plot of Δ_A versus $\ln(T)$ for samples with known areal density can serve as a calibration curve. Measuring the transmission ratio for an unknown sample, the calibration curve can be used to obtain the areal density of the unknown sample.

4.0 Coupon Standards

Five locations on twelve standard coupons of three B₄C loadings at four thicknesses each were measured. Beam port A1 was used to measure three of the five locations, while beam port A2 was used to measure the other two. Computing the transmission ratio and the areal density as described above for these measured samples, a calibration curve can be developed. This is shown in Figure 1 for each port separately. Quadratic fits of the data are also shown in the figure. The quadratic term is very small but is statistically significant. Since the curve is theoretically linear for a monoenergetic beam, the quadratic term is a measure of how non-monoenergetic the neutron beam is.

Figure 1 shows that the data is very consistent for a given port. The statistical uncertainty along the x axis for the data is slightly larger than the data points themselves. The uncertainty along the y axis is related to the uncertainty in the specified B₄C loading, the object of subsequent analysis. There is, however, a small difference between the ports. This is likely due to the ports having slightly different neutron energy spectra. Thus data from the two ports will be treated separately in subsequent analyses.

5.0 Batch 101 Specimens

To illustrate the use of the calibration curve, the areal density of each of the six Batch 101 coupons is calculated based its measured transmission ratio. The results, based on interpolating the calibration data, are given in Table 1. The small deviations in the results (all within their statistical uncertainties) further demonstrate that the experimental method is robust. It also shows that the samples all effectively have the same areal density, and thus have about the same B₄C loading (with some deviation due to differences in sample thickness).

Specimen ID	Areal Density, Δ_A	
	Port A1	Port A2
101-030	0.0112	0.0109
101-031	0.0112	0.0110
101-160	0.0110	0.0108
101-161	0.0109	0.0107
101-299	0.0110	0.0109
101-302	0.0110	0.0109
Average:	0.0110	0.0109
1 σ	0.0001	0.0001
1 σ as %	0.97%	0.93%

6.0 Repeated Measurements of a Single Location

A single location on the 24" x 4" 15% B₄C plate was measured eight times during the measurement of the plate. These measurements were distributed among all of the measurements of this plate as if these were eight distinct locations. This provides a measure of the repeatability of the measurements in order to detect any experimental error. Figure 5 shows the excellent consistency of the data, which passes all statistical tests for normality. The figure shows the transmission ratio data as points in ascending order, and ideal normal curves based on the mean and variance of the data. The difference in the mean (between the curves for each port) is as expected based on the differences noted for the calibration curves. The slopes of the curves are indicative of the variance and show that the two ports have similar variances. Table 2 shows that the observed variance is comparable to the expected variance. The fact that the observed variance is actually less than the expected variance is likely just statistical fluctuation.

	Port A1	Port A2
Expected Standard Deviation	0.30%	0.30%
Observed Standard Deviation	0.28%	0.18%

7.0 The 24" x 4" 15% B₄C Plate

The 15% plate was measured at 15 locations via port A1 and 8 locations via port 2. These measurements were smoothed across the plate to generate contour plots of the measured transmission ratio as shown in Figures 3 and 4 for ports A1 and A2, respectively. Since port A1 was vertically above port A2, port A1 measures vertical grids 3 and 4 most accurately (and tends to smooth out vertical grids 1 and 2), while port A2 measures vertical grids 1 and 2 most accurately (and tends to smooth out vertical grids 3 and 4). A multivariate linear regression analysis was performed to identify any trends in transmission ratio across the plate. A slight trend in the horizontal direction might be noted, but this is not quite statistically significant at the $V=5\%$ level of significance. The effect of such a trend will be discussed subsequently.

The transmission ratios are slightly different between the ports, as expected, but the ranges of variation are similar and very small. This is best shown in Figure 5, which is similar to Figure 2. The different slopes indicate that there is some difference between the port A1 and port A2 data for this plate, but this difference is not significant. Further, no outliers are observed. The data pass all statistical tests for normality.

Like Table 2, Table 3 compares the measured uncertainty with the expected Poisson statistical uncertainty. The locations measured by port A1 show a somewhat higher variance than expected. This may be attributable to the small non-random variation in B₄C loading horizontally across the plate, which was noted above as not being statistically significant. Whatever the cause, the increased variance is not physically significant. According to the

calibration curve, a deviation of 0.51% in transmission ratio translates to a deviation of <0.62% in areal density (<0.0003 g/cm²), a negligible effect.

	Port A1	Port A2
Expected Standard Deviation	0.30%	0.30%
Observed Standard Deviation	0.51%	0.20%

For completeness, Figure 6 shows a contour plot of the thickness across the 15% plate. The scale exaggerates the otherwise very small deviations. The thickness of the plate appears to be slightly smaller across the vertical middle of the plate. The also appears to be an “undulating” trend in the horizontal direction. For this analysis variations in the thickness were scaled out of the count rate as described previously, so these deviations have no effect on the analysis of the uniformity of the B₄C loading. Figure 7 shows that the thickness measurements are generally normal; they pass all statistical tests for normality. There is one significant deviation from the normal curve, but it is a lower than expected thickness at the large thickness end of the distribution, and so is of no practical concern.

8.0 The 22" x 14" 31% B₄C Plate

The 31% plate was measured at 14 locations via port A1 and 14 locations via port 2. These measurements were smoothed across the plate to generate contour plots of the measured transmission ratio as shown in Figures 8 and 9 for ports A1 and A2, respectively. The transmission ratios are slightly different between the ports, as expected, but the ranges of variation are similar and very small, as is shown in Figure 10. The slopes in Figure 10 are quite similar, no outliers are observed, and the data pass all statistical tests for normality.

Like Tables 2 and 3, Table 4 compares the measured uncertainty with the expected Poisson statistical uncertainty. The locations measured by both ports A1 and A2 show a higher variance than expected. This is likely attributable to small non-random variations in B₄C loading across the length of the panel. A multivariate linear regression analysis shows that there is a statistically significant increasing trend in transmission ratio (corresponding to a decrease in B₄C loading) horizontally across the plate, a trend that is clearly observable in Figures 8 and 9. There also appears to be a “trough” of low transmission ratio (high B₄C loading) in the vertical middle of the plate. Applying the regression model for the horizontal variation to the data reduces the observed variance as shown in the last row of Table 4. Port A1 is now comparable to the expected variance and port A2 is much closer. A non-linear multivariate regression that accounted for the trough in the vertical direction might bring this more in line with the expected variance. Thus the increased variance is likely due to global variations in B₄C loading across the plate, and not to local deviations. In any case, as before, whatever the cause of this small increased variance the effect is not physically significant.

Table 4: Expected And Observed Variance in Transmission Ratio For 31% Plate		
	Port A1	Port A2
Expected Standard Deviation	0.62%	0.63%
Observed Standard Deviation	1.99%	2.24%
Observed Standard Deviation After Regression	0.59%	1.16%

With respect to the thickness of the 31% plate, Figure 11 shows a contour plot of the thickness across the plate. (Note that the plate is rotated in the figure for convenient viewing.) Like the transmission ratio, there is a significant trend in thickness horizontally across the plate. Figure 12 shows that without accounting for this trend the data is clearly not normally distributed; it does not pass any of the tests for normality. Linear regression with respect to the horizontal position leads to the normally distributed residuals shown in Figure 13. This illustrates that, as for the transmission ratio, accounting for the most significant global variations shows that any local variations are negligible.

9.0 Areal Density Variation

A subset of the standards in Section 4.0 were subjected to chemical testing and a rigorous statistical analysis of the results to qualify them as standards with a known uncertainty. A methodology was developed to use these standards to develop a calibration curve with rigorously derived statistical uncertainties for predicting the areal density of unknown samples. This methodology was applied to calculate the areal density of the samples from the two plates described in Sections 7.0 and 8.0. The results are shown in Table 5.

In Table 5 the mean areal density of the samples, m , and sample standard deviation, σ , are shown in the first two rows. (Five significant figures are retained to show the results without significant rounding mismatches.) The third row shows the sample standard deviation as a percent of the mean. This is the observed areal density variance across the plate as a percent of the average observed areal density. The fourth row multiplies the sample standard deviation by the normal distribution one-sided statistical tolerance factor; the fifth row shows this as a percent of the mean. The second to last row is the one-sided normal distribution lower statistical tolerance limit on the areal density, and the last row is this limit as a percentage of the mean.

Table 5: Calculated Areal Density		
Property	15% Plate Areal Density g ¹⁰ B/cm ²	31% Plate Areal Density g ¹⁰ B/cm ²
Mean, m	0.01074	0.02196
1σ	0.00007	0.00021
1σ as % of mean	0.65%	0.96%
K _{95/95} · σ	0.00018	0.00055
K _{95/95} · σ as % of mean	1.67%	2.50%
95/95 minimum, m - K _{95/95} · σ	0.01056	0.02141
95/95 minimum as % of mean	98.3%	97.5%

There are five sources of areal density variation across a plate of METAMIC®:

- 1) uncertainty in the experimental method used other than variation due to counting statistics;
- 2) statistical uncertainty in the measurements due to the Poisson counting statistics;
- 3) variations in thickness across the plate;
- 4) non-random (global) variations in B₄C loading across the plate;
- 5) random (local) variations in B₄C loading across the plate.

The analysis of standards in Section 4.0 and repeated measurements of a single location in Section 6.0 showed that the non-counting statistics experimental uncertainty (source 1) is negligible. The statistical uncertainty (source 2) can be computed using Poisson statistics. The measured transmission ratio can be adjusted to factor out the effects of thickness (source 3); thus the contribution of thickness variation to the areal density variation can be quantified by comparing the adjusted and un-adjusted results. The global variance of B₄C loading (source 4) is determined via multiple regression analysis against horizontal and vertical plate position. The local variance (source 5) is the residual variance that is not otherwise accounted for. Table 6 shows the estimated portions of the areal density standard deviation due to these sources.

Table 6: Sources of Variance in Areal Density Measurements		
	15% Plate	31% Plate
Standard Deviation of Areal Density (Table 5, row 3)	0.65%	0.96%
Portion Due to Non-Counting Statistics Experimental Uncertainty	~0	~0
Expected Portion Due to Counting Statistics	1/3	1/4
Portion Due to Thickness Variance	1/2	1/4
Portion Due to Global B ₄ C Loading Variance	1/6	1/2
Portion Due to Local B ₄ C Loading Variance	~0	~0

The conclusion is that there is not a statistically significant random (local) variation in areal density across the plate. All of the observed variance can be attributed to the other sources indicated. A significant contributor to this variance is thickness variance. Overall, the total areal density variance is seen to be very small (less than 1%).

10.0 B₄C Loading Variation

The B₄C loading can be computed from the areal density, thickness, and material constants (e.g., constituent densities). The variance in B₄C loading eliminates the thickness variance, which was noted in Section 9.0 to be a significant contributor to areal density variance. Table 7 is identical to Table 5 except that it shows the variation in B₄C loading rather than areal density. It shows that the total variation in B₄C loading across the 15% and 31% plates is very small.

Table 7: Calculated B ₄ C Loading		
Property	15% Plate B ₄ C Loading w/o	31% Plate B ₄ C Loading w/o
Mean, m	0.1481	0.3022
1 σ	0.0005	0.0012
1 σ as % of mean	0.36%	0.41%
K _{95/95} · σ	0.0014	0.0033
K _{95/95} · σ as % of mean	0.93%	1.08%
95/95 minimum, m - K _{95/95} · σ	0.1467	0.2989
95/95 minimum as % of mean	99.1%	98.9%

11.0 Conclusions

No significant local non-uniformities in B_4C loading were observed in the plates tested. Some global non-uniformities in B_4C loading were observed, but these are very small and of no physical consequence. The thickness was also observed to have very small global trends. No significant local non-uniformities in areal density were observed in the plates tested, and the small global non-uniformities were principally attributed to the above-noted variations in thickness. After accounting for any significant global trends, the data was observed to be normally distributed, passed statistical tests for normality, and had no gross outliers.

The METAMIC[®] standards were shown to yield a consistent calibration curve with very little uncertainty. Subsequent calibration curves for the same or different incident neutron spectra are expected to accurately quantify the areal density of unknown samples.

Point-to-point variation in the areal density on both plates is very small. For the 15% plate the mean areal density is $0.01074 \pm 0.00007 \text{ g }^{10}\text{B}/\text{cm}^2$. At a 95% probability/ 95% confidence level the minimum areal density is 0.01056, or 98.3% of the mean value. For the 31% plate the mean areal density is $0.02196 \pm 0.00021 \text{ g }^{10}\text{B}/\text{cm}^2$. At a 95% probability / 95% confidence level the minimum areal density is 0.02141 $\text{g }^{10}\text{B}/\text{cm}^2$ or 97.5% of the mean.

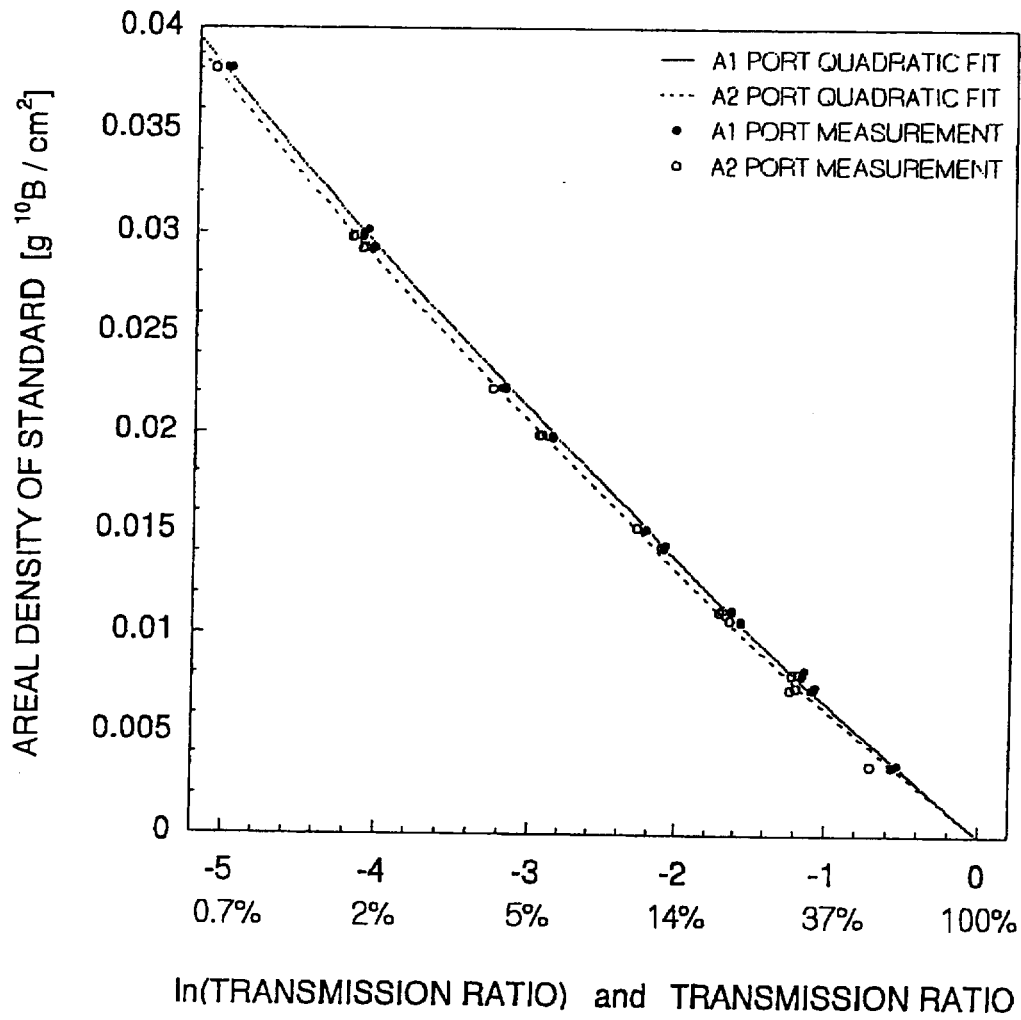


Figure 1: Calibration Curves

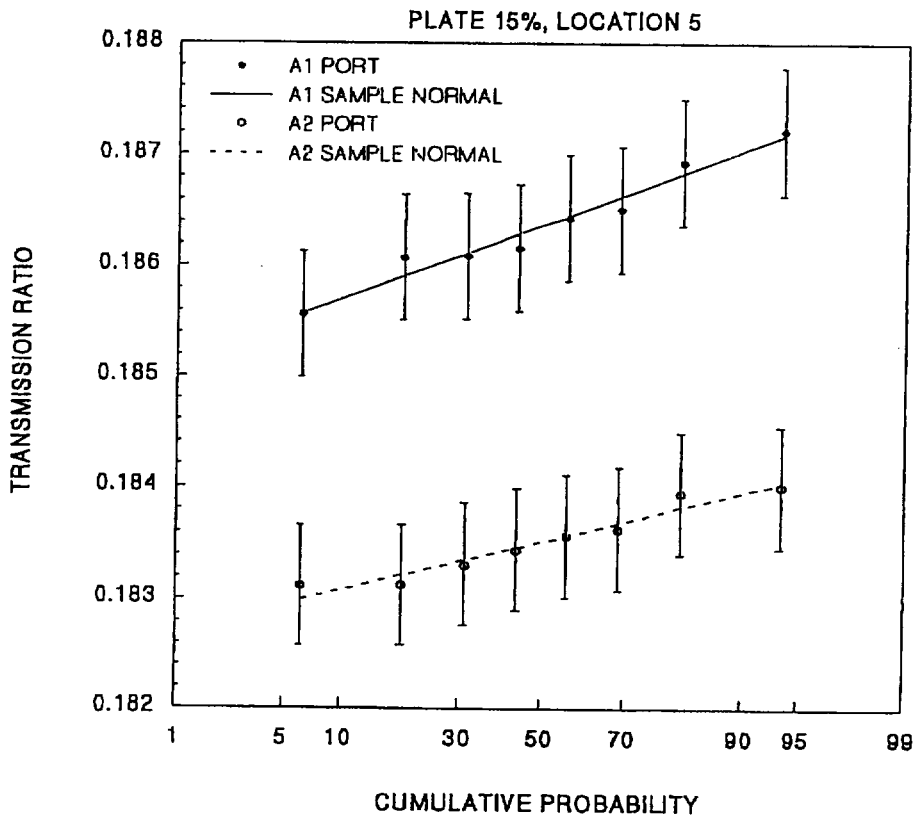


Figure 2: Normality of Transmission Ratio Data for Single Location on 15% Plate

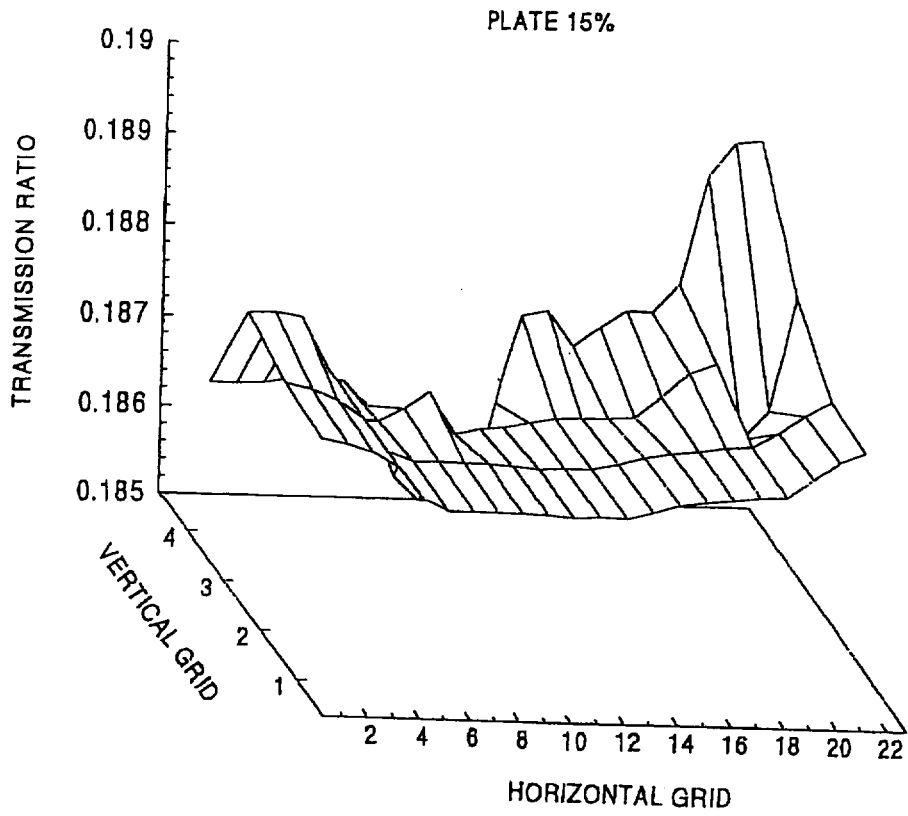


Figure 3: Transmission Ratio for 15% Plate for Port A1

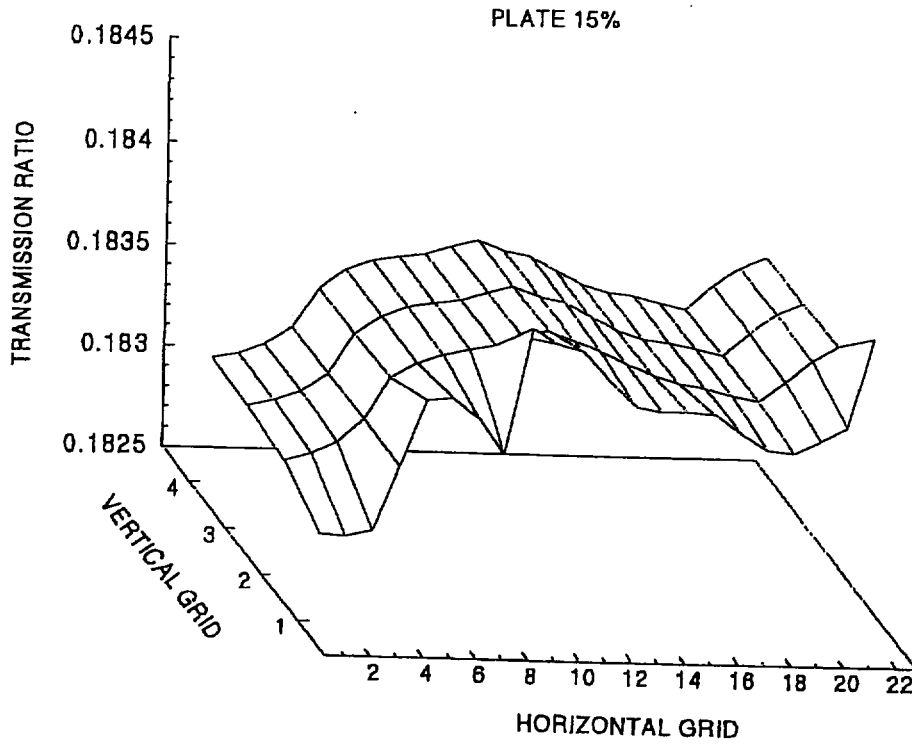


Figure 4: Transmission Ratio for 15% Plate for Port A2

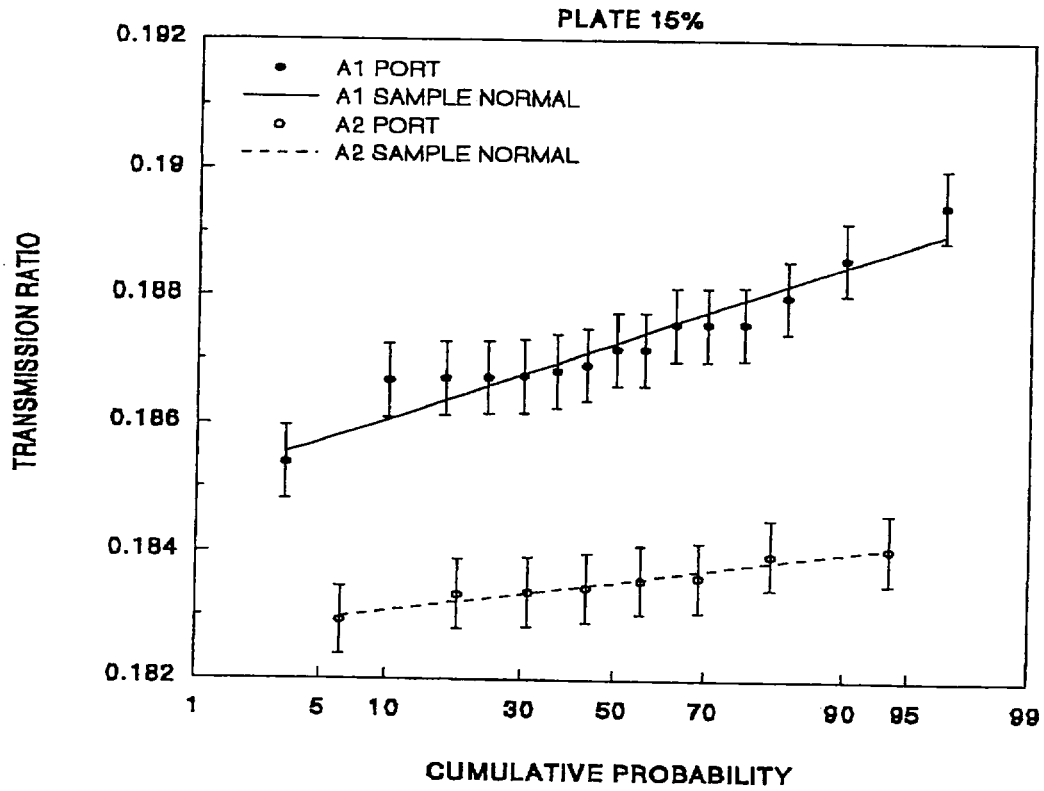


Figure 5: Normality of Transmission Ratio Data for 15% Plate

PLATE 15%

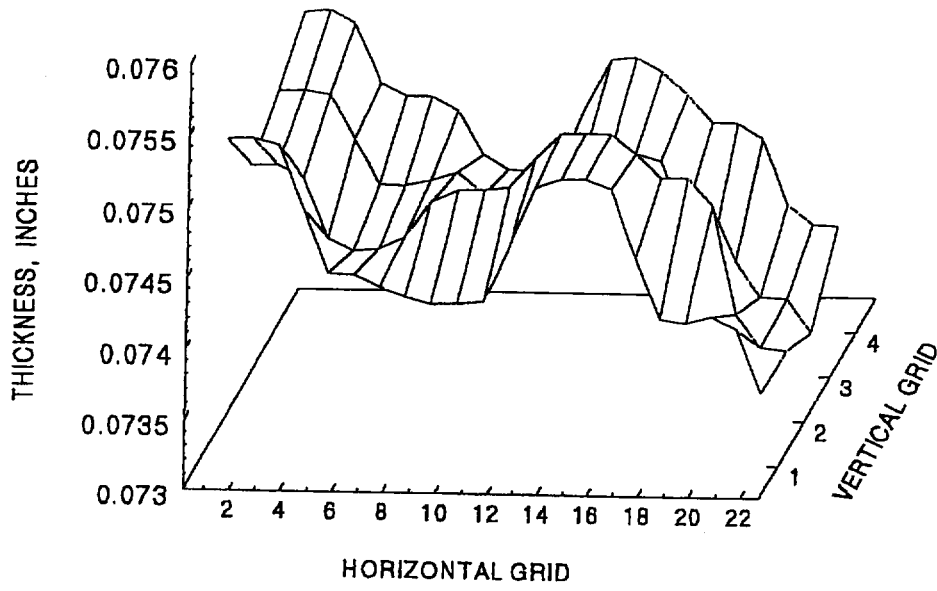


Figure 6: Thickness for 15% Plate

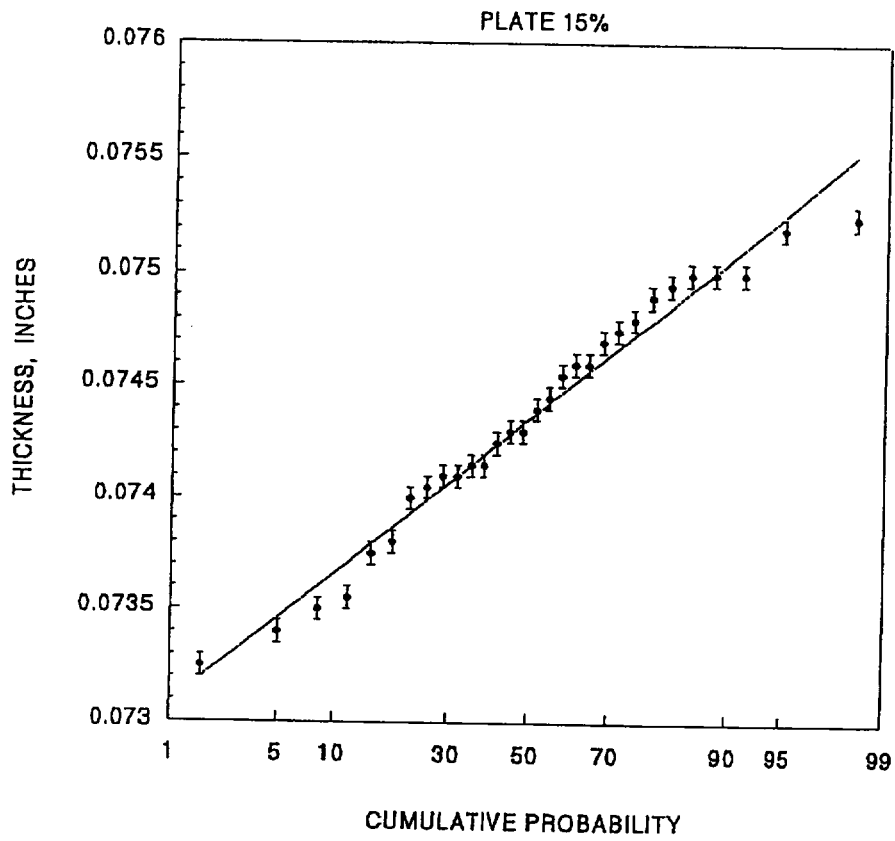


Figure 7: Normality of Thickness Data for 15% Plate

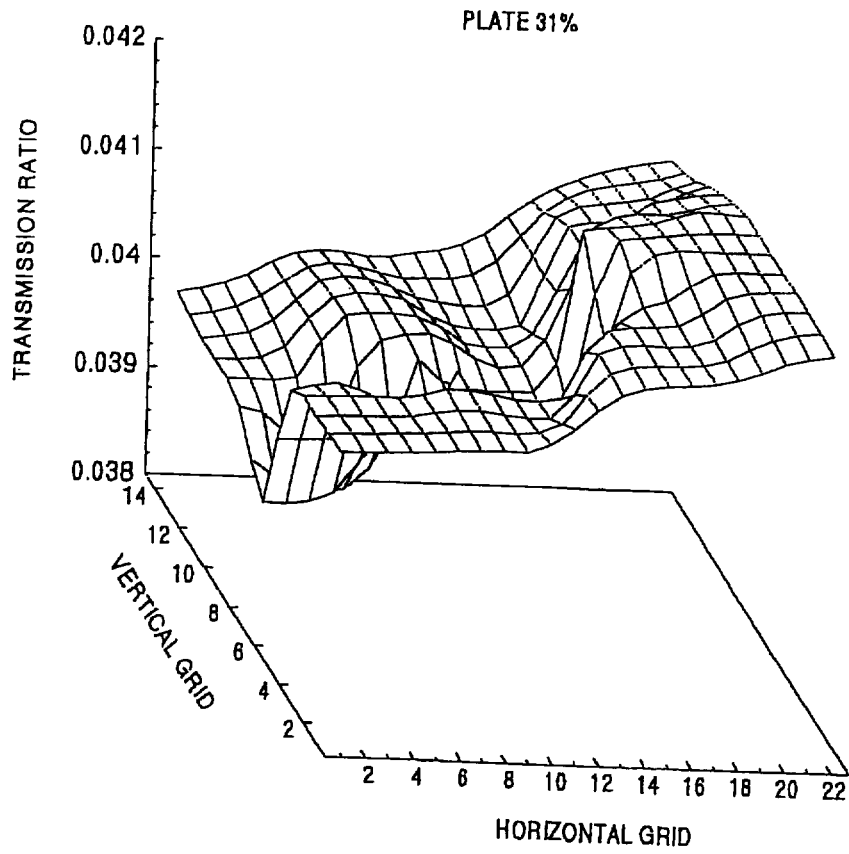


Figure 8: Transmission Ratio for 31% Plate for Port A1

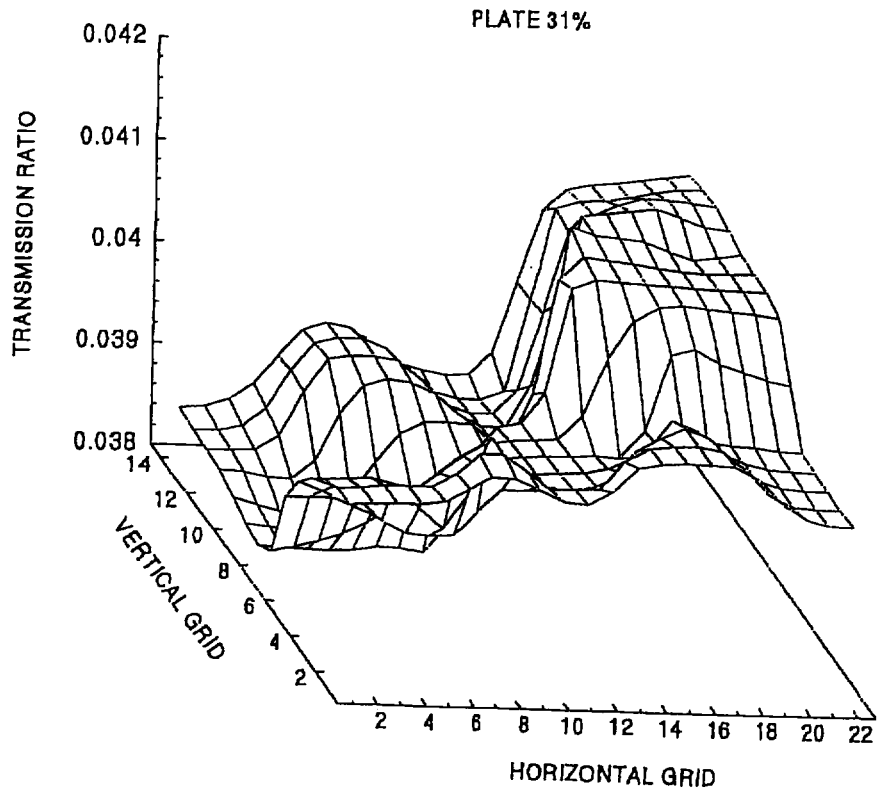


Figure 9: Transmission Ratio for 31% Plate for Port A2

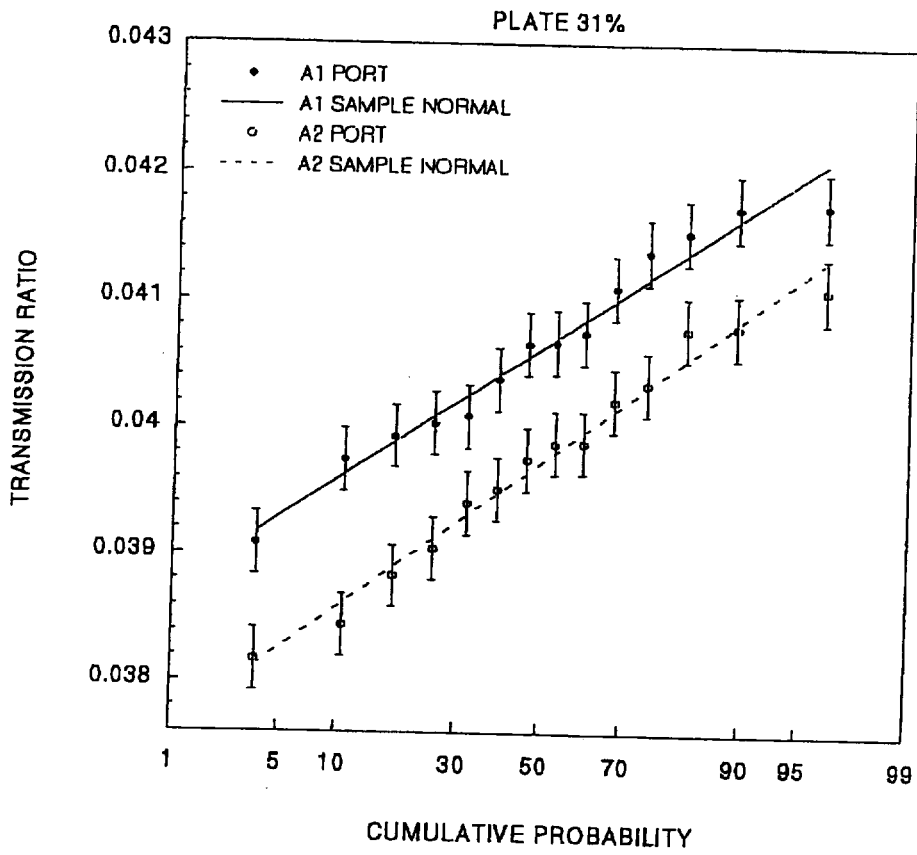


Figure 10: Normality of Transmission Ratio Data for 31% Plate

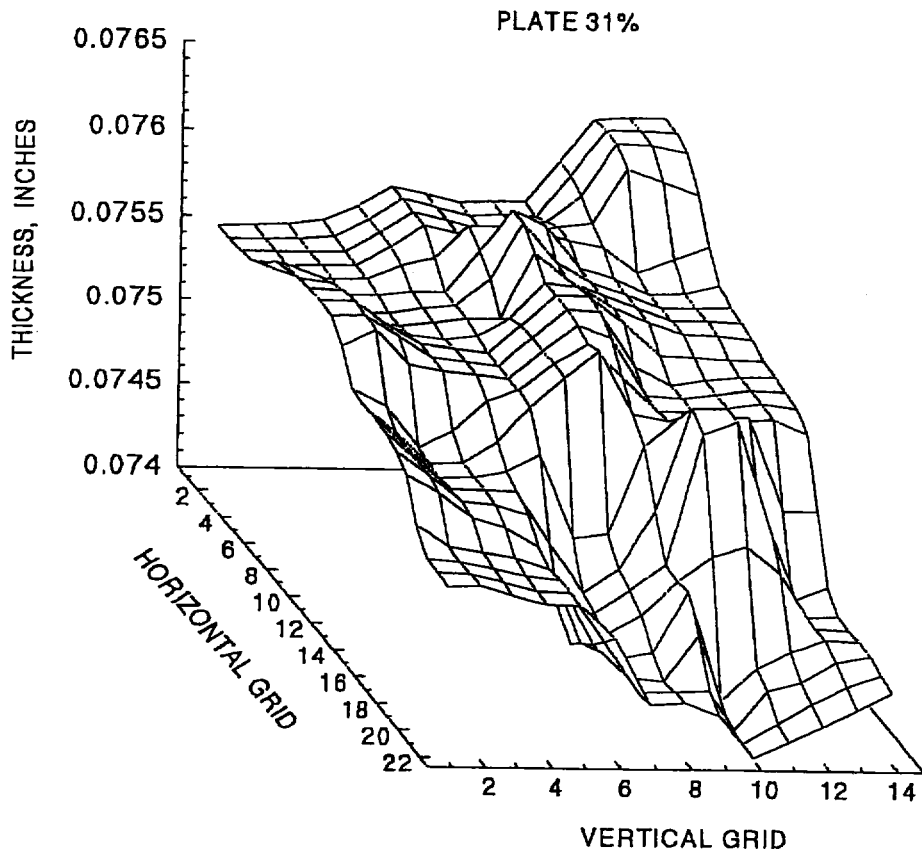


Figure 11: Thickness for 31% Plate (Rotated versus Figures 8 and 9)

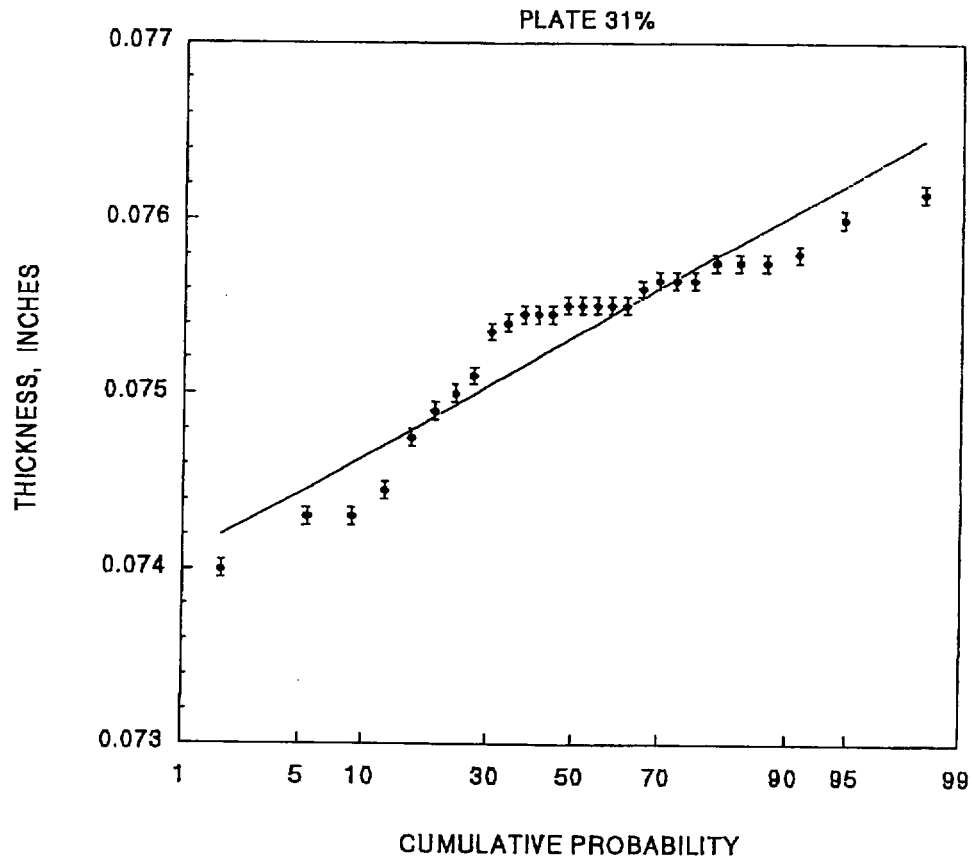


Figure 12: Normality of Thickness Data for 31% Plate